

## Donor Impurities as a Probe of Electron Correlations in a Two-Dimensional Electron Gas in High Magnetic Fields

Z. X. Jiang and B. D. McCombe

*Department of Physics, SUNY at Buffalo, Buffalo, New York 14260*

Pawel Hawrylak

*Institute for Microstructure Sciences, National Research Council of Canada,  
Ottawa, Canada K1A 0R6*

(Received 15 June 1998)

Many-electron effects have been observed in far-infrared magnetospectroscopic studies of GaAs/AlGaAs multiple quantum wells (QWs),  $\delta$  doped with Si donors in both well and barrier centers. With increasing excess electron densities in the QWs the negative donor ion ( $D^-$ ) singlet and triplet transitions are substantially blueshifted, exhibiting cusps at integer and fractional filling factors. At high magnetic fields the many-electron system appears to approach a collection of isolated two-electron  $D^-$  ions. Exact diagonalization studies of donor and confined electrons show the importance of electron correlations and localization at high magnetic fields in understanding this behavior. [S0031-9007(98)07427-4]

PACS numbers: 73.20.Dx, 73.20.Hb, 73.20.Mf, 78.66.-w

Electrons in low-dimensional semiconductor structures in a high magnetic field ( $B$ ) are strongly correlated, giving rise to a number of interesting phenomena such as the fractional quantum Hall effect, Wigner solid, and Skyrmion excitations [1]. Optical spectroscopies in strong magnetic fields have been hampered by underlying symmetries of the many-electron system which render many-electron effects invisible. The "hidden symmetry" in interband spectroscopy has been broken by either removing or localizing valence holes [2]. The better known hidden symmetry in intraband magneto-optical studies, resulting from translational invariance [3], has a limited observation of many-electron effects in cyclotron resonance (CR) studies, in which the symmetry has been broken either by disorder or by nonparabolicity of the conduction band [4]. On the other hand, for the simplest example of a many-electron system, a two-electron donor ion,  $D^-$ , far-infrared (FIR) magnetospectroscopy in bulk (3D) and quasi-two-dimensional (2D) semiconductor systems shows directly large effects of the electron-electron correlation [5–7].

Earlier studies [8,9] in which *excess* electrons were introduced into Si  $\delta$ -doped quantum wells (QWs) by stepwise modulation doping have shown that, for GaAs/AlGaAs QWs with a controlled density of randomly distributed impurities in the wells, many-electron interactions of a quasi-2DEG (two-dimensional electron gas) are rendered visible in the FIR magneto-optical spectrum. With increasing excess electron densities, the two-electron  $D^-$  singlet [5,6] and lower-energy triplet ( $T^-$ ) [7] transitions evolve continuously into blueshifted many-electron singletlike and tripletlike bound magnetoplasmon excitations. In the high density samples the singletlike transition exhibits cusps as a function of  $B$  at integral Landau level (LL) filling factors ( $\nu$ ). These results are in semiquantitative agreement with theory [10,11].

We report new results of measurements in the vicinity of  $\nu \sim 1$  and for  $\nu \ll 1$  that demonstrate the sensitivity of the donor-related FIR magneto-optical transitions to the local many-electron configuration. For  $\nu \sim 1$ , the experiments probe spin-related electron correlations, while in the regime of  $\nu \ll 1$ , they are sensitive to states of the incompressible liquid. We have observed cusps in the normalized transition energies near fractions  $\frac{1}{3}$ ,  $\frac{2}{5}$ ,  $\frac{2}{3}$ , and  $\frac{4}{3}$ . In addition, for all samples studied, the blueshift of the many-electron singletlike transition decreases with increasing  $B$  for  $\nu < 1$ , while the many-electron tripletlike transition simultaneously loses strength. The many-electron system (as many as fifteen electrons per donor) appears to approach a collection of isolated two-electron  $D^-$  ions at high enough  $B$ . Our understanding of this behavior relies on exact diagonalization studies of a few confined electrons in the presence of a donor ion. The model shows that in strong  $B$  the Coulomb potential of the positive charge attracts not one but two electrons with opposite spin (spin singlet) to its vicinity. Since this complex is charged, it repels the remaining electrons, which can move away from the  $D^-$  complex when larger (outer) orbits become available at higher  $B$  [12]. Therefore, a positive charge binding two spin-singlet electrons becomes *spatially isolated* from the remaining electrons for  $\nu \ll 1$ , and the optical properties of the many-electron system approach those of the isolated two-electron  $D^-$  singlet configuration. These studies demonstrate that many-electron singletlike and tripletlike bound magnetoplasmon excitations are sensitive to the local charge arrangement for  $\nu < 1$ .

FIR magnetospectroscopic studies were carried out with a BOMEM DA-3 Fourier transform infrared spectrometer in conjunction with 9 and 15 T superconducting magnet systems, light-pipe/condensing-cone optics, and Ge:Ga photoconductive detectors at temperatures between 1.7

and 4.2 K in the Faraday geometry. Magnetotransport measurements were performed to determine the electron density and the fields for integer and fractional filling factors. The four molecular-beam epitaxy-grown samples investigated have the same basic structure, 200 Å GaAs wells and 600 Å  $\text{Al}_{0.3}\text{Ga}_{0.7}\text{As}$  barriers repeated 20 times, all planar doped with Si donors in the well centers at  $2 \times 10^{10} \text{ cm}^{-2}$ , and planar doped in the barrier centers at  $3.5 \times 10^{10} \text{ cm}^{-2}$  (sample 1),  $8 \times 10^{10} \text{ cm}^{-2}$  (sample 2),  $1.5 \times 10^{11} \text{ cm}^{-2}$  (sample 3), and  $2.8 \times 10^{11} \text{ cm}^{-2}$  (sample 4). Sample 1 has been intensively studied [6–9] and serves as a reference sample for the many-electron effects observed in the higher excess electron density samples.

Magnetotransmission spectra for sample 3 are shown in Fig. 1. The major features at 4.2 K are CR at  $121 \text{ cm}^{-1}$  [The CR lines for all of the other spectra at different fields are aligned to this position to clearly show the behavior of the other feature(s)], and a many-electron singletlike line at  $166 \text{ cm}^{-1}$  at 9 T, blueshifted by  $6\text{--}7 \text{ cm}^{-1}$  at 9 T from the position (indicated by the downward arrow) of the isolated two-electron  $D^-$ -singlet line of sample 1 [9]. In addition, the many-electron tripletlike line is observed at about 7 T as a weak shoulder on the low frequency side of the broadened (due to overabsorption) CR. It is apparent that the strength of this tripletlike line *decreases* with increasing  $B$ , *opposite* to the behavior of the tripletlike line of sample 4 over the magnetic-field range studied [9];

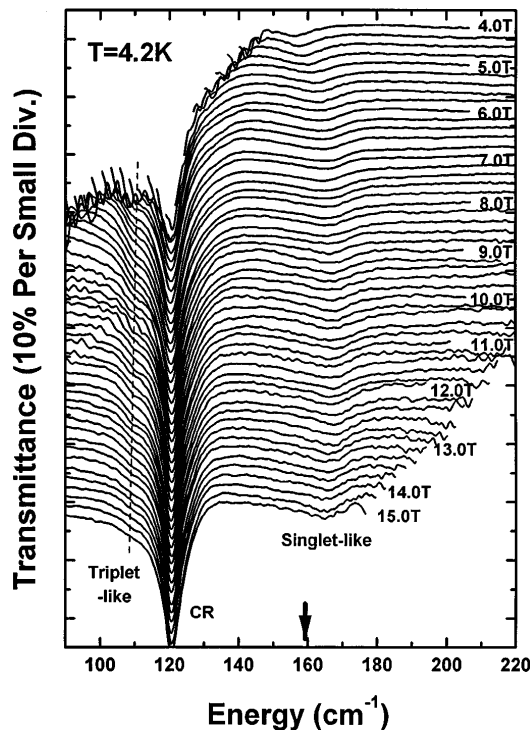


FIG. 1. Magnetotransmission spectra for sample 3 at 4.2 K in magnetic fields between 4 and 5 T in steps of 0.25 T, between 5 and 14 T in steps of 0.2 T, and at 14.5 and 15 T. The CR lines for spectra at different fields are aligned to the CR position of the 9 T spectrum. The downward arrow indicates the position of the isolated two-electron  $D^-$ -singlet line for sample 1 at 9 T.

over this range (7–15 T),  $0.87 \leq \nu \leq 1.67$  for sample 4, whereas  $0.41 \leq \nu \leq 0.89$  for sample 3. This suggests that the strength of the tripletlike transition depends on  $\nu$ ; with increasing  $B$  for  $\nu \ll 1$  the many-electron tripletlike transition behaves like the isolated two-electron  $D^-$ -triplet ( $T^-$ ) line, i.e., it is not observable at low temperature [7]. Similar behavior has also been observed for sample 2.

A summary of the energy shifts of singlet (sample 1) and singletlike (samples 2–4) resonance positions from CR plotted vs  $B$  is presented in Fig. 2. The substantial and systematic blueshift of the many-electron singletlike bound magnetoplasmon data of samples 2, 3, and 4 relative to the two-electron  $D^-$ -singlet data of sample 1 is apparent; the largest shift occurs for sample 4 (solid circles) and the smallest for sample 2 (solid triangles). There are clear breaks in the slope for both samples 3 and 4, just over 6 T and near 12.5 T for sample 3 and just below 6 T and about 11.5 T for sample 4. Note also that the singletlike transition energies of samples 2, 3, and 4 approach those of the isolated two-electron  $D^-$ -singlet line of sample 1 when  $\nu < 1$ , and the rate of approach increases with excess electron density (the largest for sample 4 and the smallest for sample 2). The underlying physics of this systematic behavior is the focus of the following discussion.

To examine these results more closely the data for samples 2 and 3 are replotted in Fig. 3(a) and the data for all samples 2–4 in Fig. 3(b), respectively, as energy differences between the many-electron singletlike and the

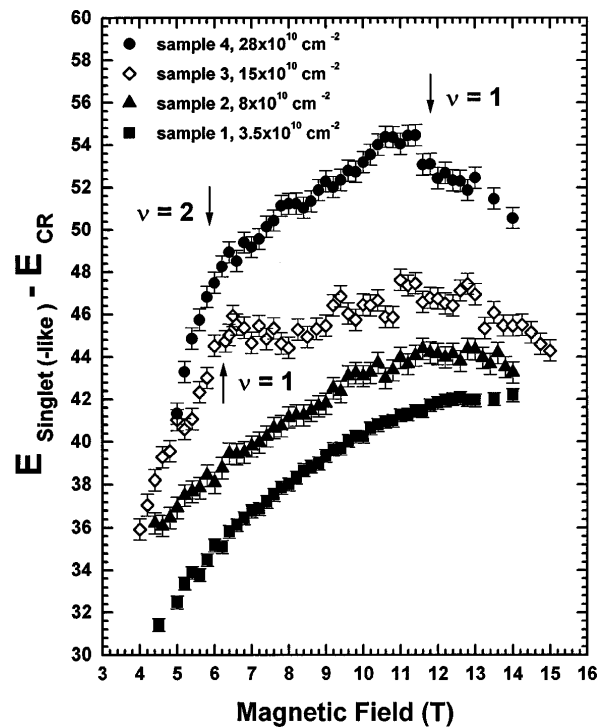


FIG. 2. Energy shifts of resonance positions from CR vs  $B$  for the two-electron  $D^-$ -singlet transition (■) of sample 1 and for the many-electron singletlike transitions of samples 2 (▲), 3 (◇), and 4 (●). The data of sample 3 for  $B \leq 9$  T were taken at  $T = 1.7$  K, all others at 4.2 K.

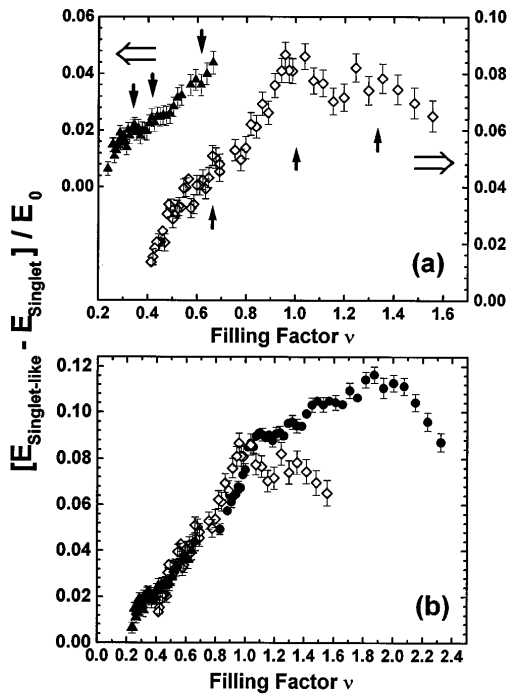


FIG. 3. Energy differences between the many-electron singletlike magnetoplasmon and the isolated two-electron  $D^-$ -singlet transitions normalized by the binding energy of a 2D neutral donor in the high- $B$  limit vs  $\nu$  (a) for samples 2 ( $\blacktriangle$ ) and 3 ( $\diamond$ ), and (b) for all samples 2 ( $\blacktriangle$ ), 3 ( $\diamond$ ), and 4 ( $\bullet$ ).

two-electron  $D^-$ -singlet transitions normalized by the  $B$ -dependent binding energy of a 2D neutral donor in the high-field limit,  $E_0 = (\pi/2)^{1/2}(e^2/\epsilon\ell) = (\pi/2)^{1/2}E_{Coul}$ , with  $\epsilon$  the background dielectric constant,  $\ell = (\hbar c/eB)^{1/2}$  the magnetic length, and  $E_{Coul}$  the high-field Coulomb energy. In addition to the sharp cusplike feature near  $\nu = 1$ , discussed in [9], the data for sample 3 in Fig. 3(a) show cusps near the fractions  $\frac{2}{3}$  and  $\frac{4}{3}$ , and for sample 2 cusps are seen near  $\frac{2}{3}$ ,  $\frac{1}{3}$ , and possibly  $\frac{2}{5}$ . It is also apparent that the normalized shifts are approximately the same, where they overlap. For  $\nu < 1$  the scaling among the blueshifts for all three samples is illustrated in Fig. 3(b). All of the apparently different shifts and rates of approach in Fig. 2 are seen to collapse onto a single curve in this scaled plot; this clearly demonstrates their common origin in the many-electron interactions.

As mentioned above, for all samples studied the blueshift of the many-electron singletlike transition decreases with increasing  $B$  for  $\nu < 1$  [Figs. 2 and 3(b)], while the many-electron tripletlike transition simultaneously loses strength (Fig. 1). From the perspective of the optical transitions, the many-electron system approaches a collection of isolated two-electron  $D^-$  ions at high enough  $B$ . To understand the essential physics of this behavior, we have performed exact diagonalization studies of a few electrons in a confining potential with a positive charge at the origin [13]. In our model, the positive background charge and confining edges are simulated by a parabolic confining potential in the radial direction of the QW

plane. The single particle states  $|m\sigma\rangle$  are the lowest LL orbitals with  $m$  the angular momentum projection along the  $B$  direction, and spin  $\sigma = +\frac{1}{2}$  (spin up) and  $-\frac{1}{2}$  (spin down). The many-electron Hamiltonian is diagonalized exactly in the space of many-electron configurations [13]. The choice of lowest LL orbitals is such that at  $\nu = 1$ , there are ten states available for nine spin-up electrons.

Figure 4 shows the calculated charge distribution vs  $m$  for the lowest LL in three cases. In case (a),  $\nu > 1$ , the state consists of a droplet of spin-polarized spin-up electrons (lower panel), and a spin-down electron with  $m = 0$  localized on the donor (upper panel). With increasing  $B$  (decreasing  $\nu$ ), empty states (holes) become available to accommodate unpaired spin-up electrons. Without a donor the electrons would form a spin-up polarized droplet. The donor potential changes this behavior, and the ground state corresponds to a spin-down electron in the presence of spin-up electrons. It has been shown [11] that a many-electron system in the absence of a confining potential with a fixed positive charge (and very small Zeeman energy) has a lower energy if one spin-up electron is removed from the  $m = -1$  orbital state and placed in the empty spin-down state with  $m = 0$ , because the gain of negative potential energy in the field of the donor is larger than the loss of spin flip (Zeeman) and exchange energies. The strong Coulomb potential of the positive charge always attracts two spin-singlet electrons to its vicinity, and the ground state at  $\nu = 1$  is then a “spin-wave” state. This type of state for the present case [Fig. 4(b)] consists approximately of a spin singlet (at  $m = 0$ ) and a hole (in the  $m = -1$  state), rather than the (unstable) spin-polarized state, in which

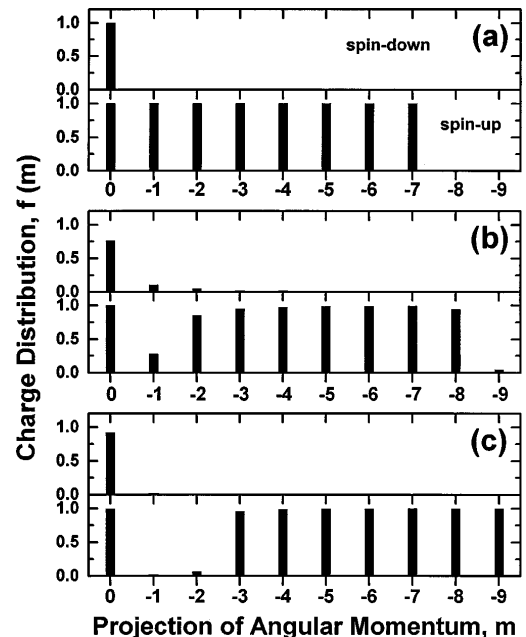


FIG. 4. The calculated electron charge distribution vs  $m$  for the lowest LL for the model described in the text; (a)  $\nu > 1$ , (b)  $\nu = 1$ , and (c)  $\nu < 1$ . Each of the upper and lower panels are for spin-down and spin-up electrons, respectively.

nine spin-up electrons occupy the inner states, leaving a hole (the last empty state) on the edge. The holes appearing in the  $\nu = 1$  state cause spin depolarization (spin textures) only when sufficiently far away from the donor; the spin textures do not significantly affect the charge distribution close to the donor (or the singletlike transition energy). More importantly for the present study, exact diagonalization shows that additional holes, which become available by further increasing  $B$  for  $\nu < 1$ , tend to move into the vicinity of the spin-singlet/hole complex. The remaining electrons move to larger (outer) orbits as they become available at higher  $B$  to maximize their separation, decrease the electron-electron repulsion, and minimize the total energy [see Fig. 4(c)]. Therefore a positive charge binding two spin-singlet electrons becomes *spatially isolated* from the remaining electrons for  $\nu \ll 1$ , and the optical properties of the many-electron system approach those of the isolated two-electron  $D^-$ -singlet configuration. The many-electron tripletlike transition decreases in strength, because the state with  $m = -1$  (the initial state of the transition) becomes depopulated even at 4 K. Details of the calculations, including the fractional regime, will be presented elsewhere [13].

This model is justified physically by the existence of long-range, disorder potential fluctuations in the QW plane caused by randomly distributed remote dopant impurity ions. When the magnetic length,  $\ell = 256 \text{ \AA}/[B]^{1/2}$  becomes significantly smaller than the correlation length ( $\ell_C \sim 400 \text{ \AA}$ ) [14] of the fluctuating potential (at high  $B$ ), electrons tend to localize first in the lowest and widest potential minima. Since the average distance between donors in the QW plane at a density of  $2 \times 10^{10} \text{ cm}^{-2}$  is  $700 \text{ \AA}$ , the probability of a donor ion in the center of the well being located laterally near the center of a fluctuating potential minimum is significant. Given these considerations we believe that the essential physics of the simple model can be applied to the experimental observations, and the results are in good qualitative agreement with the experiments in the region of  $\nu < 1$ .

In summary, we have shown that FIR magneto-optical transitions associated with donor impurities can be used to probe many-electron effects in a surrounding 2DEG, and that these excitations of the system depend sensitively on the microscopic electron configuration in the vicinity of the positive donor ions. Filling-factor-dependent energy shifts of the many-electron singletlike transition are observed in the integer and fractional quantum Hall regime, and for all samples studied the blueshift of this transition decreases with increasing  $B$  for  $\nu < 1$ , while the many-electron tripletlike transition simultaneously loses strength. The many-electron system appears to approach a collection of isolated two-electron  $D^-$  ions at high enough  $B$ . The physics of the high-field behavior is revealed by exact diagonalization studies of a donor and electrons in a

parabolic confining potential, which show that for  $\nu < 1$  electron-electron correlations tend to isolate a pair of spin-singlet electrons at the position of the positive charge with the additional confined electrons moving away toward the confining edge to minimize the Coulomb repulsion. This yields the observed optical response. The sensitivity of the magneto-optical transitions to electron-electron correlations (and the resulting local electron configuration) underlies the anomalies at fractional filling factors.

The excellent multiple QW samples were grown by W. Schaff at Cornell University. This work was supported in part by the ONR/MFEL Program under Grant No. N00014-97-10858 and by NSF under Grant No. DMR-962409.

- 
- [1] L. Brey, H.A. Fertig, R. Côte, and A.H. MacDonald, Phys. Rev. Lett. **75**, 2562 (1995).
  - [2] See, for example, L. Gravier, M. Potemski, P. Hawrylak, and B. Etienne, Phys. Rev. Lett. **80**, 3344 (1998); E.H. Aifer, B.B. Goldberg, and D.A. Broido, Phys. Rev. Lett. **76**, 680 (1996).
  - [3] W. Kohn, Phys. Rev. **123**, 1242 (1961).
  - [4] See, for example, M. Besson *et al.*, Semicond. Sci. Technol. **7**, 1274 (1992); G.M. Summers *et al.*, Phys. Rev. Lett. **70**, 2150 (1993); N.R. Cooper and J.T. Chalker, Phys. Rev. Lett. **72**, 2057 (1994).
  - [5] See, for example, S. Huant, S.P. Najda, and B. Etienne, Phys. Rev. Lett. **65**, 1486 (1990); E.R. Mueller, D.M. Larsen, J. Waldman, and W.D. Goodhue, Phys. Rev. Lett. **68**, 2204 (1992).
  - [6] S. Holmes, J-P. Cheng, B.D. McCombe, and W. Schaff, Phys. Rev. Lett. **69**, 2571 (1992).
  - [7] S.R. Ryu, Z.X. Jiang, W.J. Li, and B.D. McCombe, Phys. Rev. B **54**, R11086 (1996); S.R. Ryu, W.-Y. Yu, L.P. Fu, Z.X. Jiang, A. Petrou, B.D. McCombe, and W. Schaff, Surf. Sci. **361/362**, 363–367 (1996).
  - [8] J-P. Cheng, Y.J. Wang, B.D. McCombe, and W. Schaff, Phys. Rev. Lett. **70**, 489 (1993).
  - [9] Z.X. Jiang, S.R. Ryu, and B.D. McCombe, Semicond. Sci. Technol. **11**, 1608 (1996); Z.X. Jiang, B.D. McCombe, and P. Hawrylak, in *Proceedings of the 23rd International Conference on the Physics of Semiconductors, Berlin, Germany* (World Scientific, Singapore, 1996), Vol. 3, p. 2535.
  - [10] A.B. Dzyubenko and Yu.E. Lozovik, JETP Lett. **77**, 617 (1993).
  - [11] P. Hawrylak, Phys. Rev. Lett. **72**, 2943 (1994).
  - [12] R.C. Ashoori, Nature (London) **379**, 413 (1996), and references therein.
  - [13] P. Hawrylak and W. Czart (to be published); A. Wojs and P. Hawrylak, Phys. Rev. B **56**, 13227 (1997).
  - [14]  $\ell_C \sim \ell_{BW}$  (400 Å), the distance between the barrier donor sheet and the QW center, when  $\ell_{BW} \geq$  the average barrier-donor separation. For barrier doping densities  $(8-28) \times 10^{10} \text{ cm}^{-2}$ , this average separation is 350–187 Å.